journal

J. Am. Ceram. Soc., 87 [7] 1354–1357 (2004)

# Sintering in Nitrogen Atmosphere of Iron-Rich Glass-Ceramics

Alexander Karamanov, Giuliana Taglieri, and Mario Pelino*

Department of Chemistry, Chemical Engineering and Materials, University of L'Aquila, 67040 Monteluco di Roio, L'Aquila, Italy

**The sintering and the crystallization of two iron-rich glass compositions (45–75-μm powder fractions) were studied in air and nitrogen atmospheres. The phase formation was evaluated by differential thermal analysis, while the densification, by dilatometry; the crystalline phases were identified by X-ray diffraction and the structure observed by scanning electron microscopy. It was highlighted that, due to the absence of $Fe^{2+}$ oxidation and lower viscosity of the parent and residual glasses, the sintering in nitrogen atmospheres occurs at 100°–200°C lower temperature. In the same time the higher amount of crystal phase, formed during sinter–crystallization in inert atmosphere, improves the mechanical properties. A value of 120 MPa for the bending strength was obtained after 1-h sintering at 960°C in $N_2$.**

## I. Introduction

IRON in glasses can be present in the form of $Fe^{2+}$ and $Fe^{3+}$; the $Fe^{3+}/Fe^{2+}$ ratio depends on the initial chemical composition and on the melting conditions.[1–3] In the iron-rich glass compositions obtained from industrial wastes, without addition of reducing agents during melting, $Fe^{3+}/Fe^{2+}$ usually ranges between 6 and 8.[4] Similar values were found in molten basalts[5,6] and in glasses developed for electronic applications,[7] melted in the 1350°–1400°C range.

In the amorphous glass structure the FeO acts as a modifying oxide while $Fe_2O_3$ is usually considered as an intermediate; therefore, by increasing the $Fe^{3+}/Fe^{2+}$ ratio, the viscosity will also increase. However, the iron oxides have limited solubility in silicate melts, and the iron-rich glasses show a spontaneous liquid immiscibility.[8–11] One of the formed liquid phase is richer in iron oxides and promotes the formation and precipitation of the magnetite spinels ($FeO{\cdot}Fe_2O_3$). The trend of spontaneous magnetite formation is higher the closer the $Fe^{3+}/Fe^{2+}$ ratio is to the stoichiometric value.[4,5] The formed magnetite crystals act as nuclei for the precipitation of the pyroxene phase.[5,8–11] The formation of different liquid and crystal phases increases the apparent viscosity of the melt,[12,13] which might result in difficulties during the shaping and forming processes.[14] By heating the glasses above the glass-transformation range, the oxidation of $Fe^{2+}$ to yield $Fe^{3+}$ might take place, producing, by a complex mechanism, the variation of the chemical compositions of the surface and subsurface layers.[15–18]

In a previous work,[19] the sintering in air atmosphere was investigated for two powdered glass compositions having different crystallization trends. It was shown that the crystallization of the glass inhibits the densification and increases the sintering temperature. On the other hand, the morphology of the residual porosity (closed or open) depended on the amount of crystal phase formed.

The sintering and crystallization of the same compositions were, later, studied in $N_2$ atmosphere, and the results are reported in the present work and compared with ones obtained in air.

## II. Experimental Procedure

The chemical compositions of the parent glasses (labeled G1 and G2) are reported in Table I. They were obtained by mixing jarosite, a hazardous residue from the hydrometallurgy of zinc and granite powder from ornamental stone production. The batch was melted in a pilot-scale melting kiln at 1400°C. The melting experimental procedure is reported elsewhere.[19]

The "green" samples ($10 \times 4 \times 4$ mm$^3$ size) were prepared by mixing the 45–75-μm powder fractions with a 7% polyvinyl alcohol (PVA) solution and by pressing at 100 MPa. After drying and a preliminary 30-min step at 280°C (to eliminate the PVA), the samples were treated in air and nitrogen atmospheres (1 L/min $N_2$ flow) in a "Netzsch 402 ED" differential dilatometer at 5°C/min.

The crystallization process was evaluated by means of differential thermal analysis (DTA; "Netzsch STA 409" apparatus) using about 120 mg of powder sample (45–75-μm particle size) at 5°C/min heating rate.

The percentage of crystalline phase was determined by X-ray diffraction (XRD) technique, using a Philips-1830 apparatus and Cu*K*α radiation, and comparing the amorphous halo in the glass-ceramic to the one of the corresponding parent glass at $2\theta = 25°$, 28°, and 33°.[20]

The degree of sintering and the structure of the final glass-ceramics were examined on the fractured surface by scanning electron microscopy (SEM; Philips XL30CP), while the crystal morphology was observed by backscattered electrons (BSE) after polishing of samples.

Series of five samples (initial size of $50 \times 4 \times 4$ mm$^3$) were sintered in air and nitrogen atmospheres at 5°C/min heating rate and 1-h isothermal step at different temperatures, as listed in Table II. The bending strength was determined by a three-point bending test with 40-mm outer span and a speed of 0.1 mm/min (SINTEC D/10). The Young modulus was determined by means of the nondestructive resonance frequency technique (Grindosonic).

## III. Results and Discussion

The sintering dilatometric curves of G1 and G2 in air (labeled G1-air and G2-air) are depicted in Fig. 1 and Fig. 2, together with

**Table I. Chemical Compositions of the Investigated Glass Compositions G1 and G2**

| | $SiO_2$ | $Al_2O_3$ | $Fe_2O_3$† | CaO | ZaO | PbO | $K_2O$ | $Na_2O$ | Other |
|---|---|---|---|---|---|---|---|---|---|
| G1 | 47.7 | 5.6 | 18.9 | 6.8 | 4.6 | 0.5 | 2.2 | 10.3 | 2.1 |
| G2 | 42.9 | 5.8 | 25.2 | 9.6 | 5.6 | 0.7 | 2.1 | 6.5 | 1.1 |

†Iron oxides are presented as $Fe_2O_3$.

J. Alarcon—contributing editor

Manuscript No. 10289. Received June 6, 2003; approved January 27, 2004.
*Member, American Ceramic Society.
†Author to whom correspondence should be addressed. e-mail: karama@ing.univaq.it; pelino@ing.univaq.it.

**Table II. Sintering Temperatures, Liner Shrinkage, and Mechanical Properties of the Obtained Sintered Glass-Ceramics**

| | Sintering temperature (°C) | Linear shrinkage (%) | Young's modulus (Gpa) | Bending strength (MPa) |
|---|---|---|---|---|
| G1-air | 970 | 11.7 ± 0.3 | 66 ± 2 | 73 ± 12 |
| G1-$N_2$ | 760 | 12.6 ± 0.2 | 72 ± 3 | 91 ± 8 |
| G2-air | 1050 | 11.5 ± 0.2 | 78 ± 4 | 83 ± 9 |
| G2-$N_2$ | 960 | 12.2 ± 0.3 | 80 ± 4 | 122 ± 6 |

the corresponding DTA traces; in Fig. 3 and Fig. 4 are presented the results obtained in $N_2$ atmosphere (labeled G1-$N_2$ and G2-$N_2$, respectively).

The DTA traces highlighted the typical behavior of iron-rich glass powders, heat-treated in air and $N_2$.[9,21] G1-air and G2-air show wide exoeffects in the range 600°–750°C, due to $Fe^{2+}$ oxidation as well as the crystallization peaks with the maximum at 815° and 840°C for G1-air and G2-air, respectively. In nitrogen atmosphere, no oxidation is evident and the crystallization takes place at 785°C for G1-$N_2$ and at 750°C for G2-$N_2$. The stronger intensity of the peaks showed by $N_2$-treated samples are due to the higher rate and percentage of crystallization.[21]

In the previous work conducted in air,[19] the sintering of G1 and G2 was evaluated by the linear shrinkage measured after 1-h sintering at different temperatures. It was shown that, up to 850°C for G1 and up to 900°C for G2, the sintering process is inhibited by the crystalline-phase formation and the shrinkage ranged between 4% and 6%; above those temperatures, the densification increased as a function of temperature. These previous results are confirmed by the dilatometric curves presented in Fig. 1 and Fig. 2, where the shrinkage increases up to 800°C (reaching about 8% for G1-air and about 6% for G2-air) and then stops in the crystallization interval. At about 900°C for G1-air and at 950°C for G2-air an increase in the $\Delta L/L_o$ (%) is evident due to the decreasing of the apparent viscosity as a function of the temperature.

In $N_2$ atmosphere, the sintering occurs at lower temperatures and with a different behavior for G1-$N_2$ and G2-$N_2$. In G1-$N_2$ (Fig. 3), the sintering starts at about 600°C and the densification is concluded before the beginning of the crystalline-phase formation; at 700°C the shrinkage is more than 10%, and at 750°C some deformations were observed in the sample due to force applied by the dilatometer push rod. In the same temperatures, the shrinkage in G1-air is about 1% at 700°C and about 5% at 750°C; then the sintering rate starts to decrease as a result of the beginning of the crystallization. The higher sintering rate and densification of G1-$N_2$ compared with those of G1-air are explained by the lower viscosity of the glass due to the absence of $Fe^{2+}$ oxidation in inert atmosphere.

The sintering behavior of G2 in air and $N_2$ is rather complex. The densifications in nitrogen starts at lower temperature and at 700°C the shrinkage is 2.5% and 0.5% for G2-$N_2$ and G2-air, respectively. However, at 720°C in G2-$N_2$ an intensive crystallization process starts which inhibits the densification, while in G2-air, as a consequence of the oxidation process, the phase formation starts at 810°C. As a result, at 800°C the shrinkage is 3% for G2-$N_2$ and 5% for G2-air. By increasing the temperature, the sintering behavior varies again: due to the lower viscosity of the

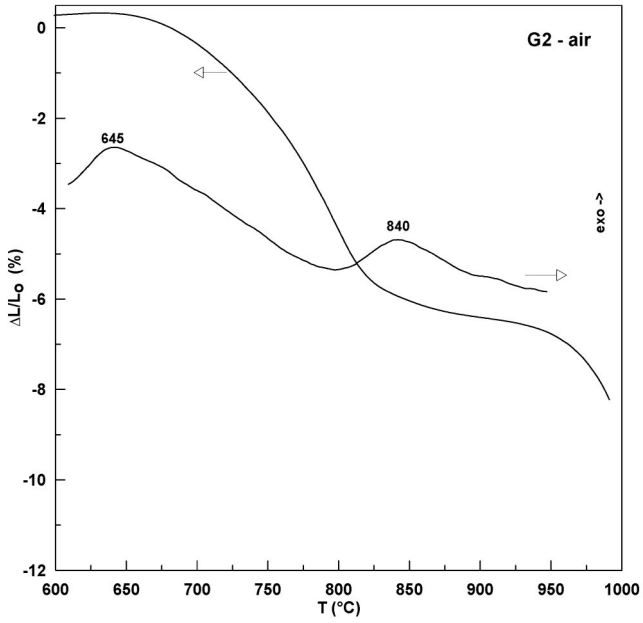


**Fig. 2.** Dilatometric sintering curve and DTA trace of G2-air at 5°C/min.

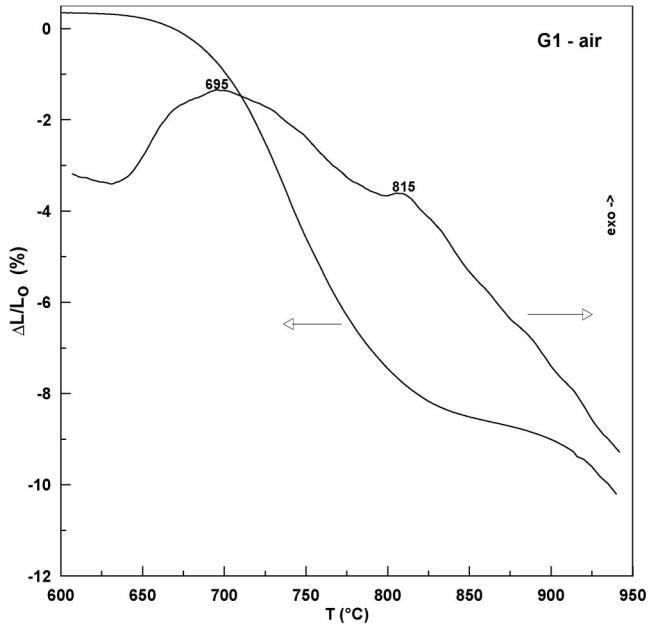


**Fig. 1.** Dilatometric sintering curve and DTA trace of G1-air at 5°C/min.

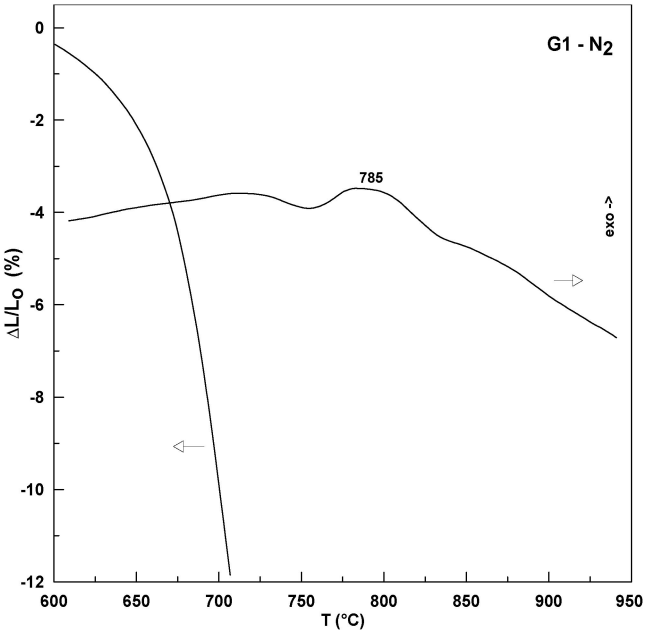


**Fig. 3.** Dilatometric sintering curve and DTA trace of G1-$N_2$ at 5°C/min.

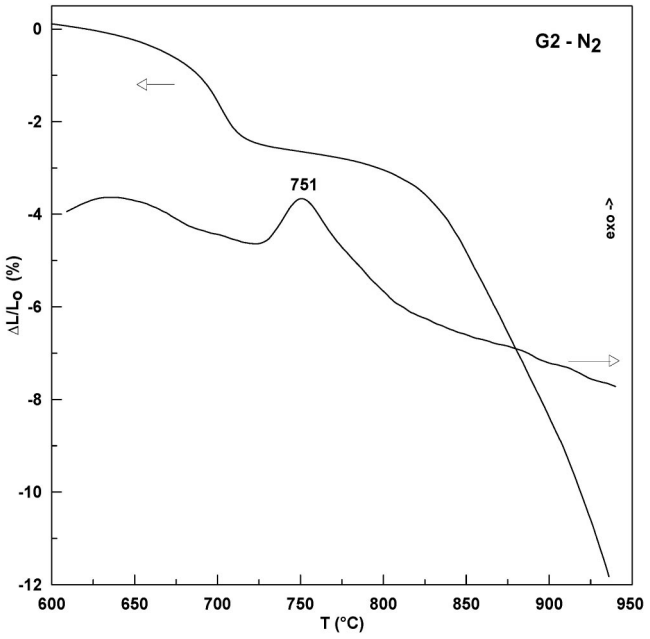


**Fig. 4.** Dilatometric sintering curve and DTA trace of G2-$N_2$ at 5°C/min.

residual glass, the densifications in G2-$N_2$ restart at 850°C, while the same phenomenon occurs at 950°C in G2-air.

The oxidation produces a change of color in the sintered glass-ceramics; i.e., in nitrogen atmosphere the samples are black, while in air they become red-brown. The black color is due to the simultaneous presence of $Fe^{2+}$ and $Fe^{3+}$ ions, while the red-brown is due to the $Fe^{3+}$ ion only.[1,3] The same colors are shown by the corresponding crystalline phases, i.e., magnetite ($FeO{\cdot}F_2O_3$) and hematite ($Fe_2O_3$).[22]

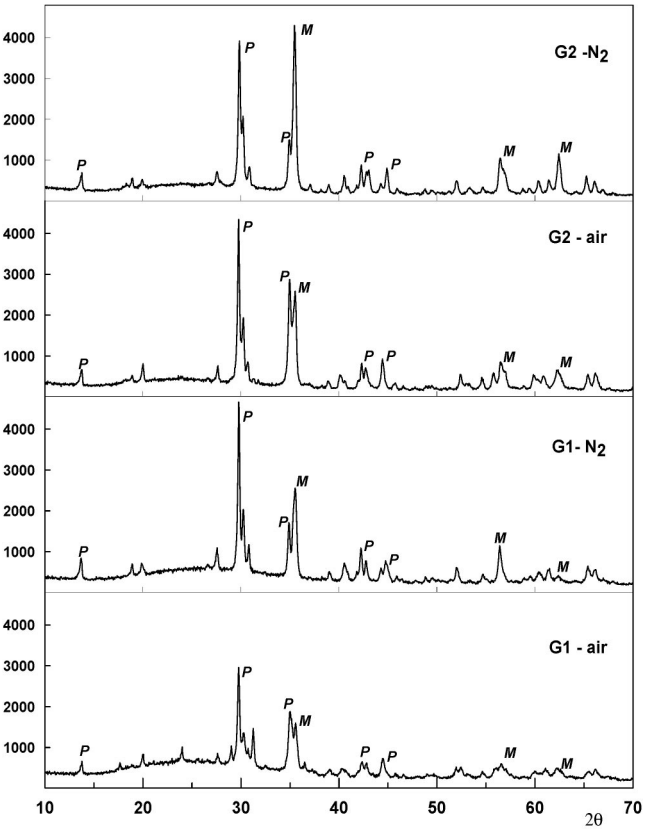


**Fig. 5.** XRD spectra of the sintered glass-ceramics.

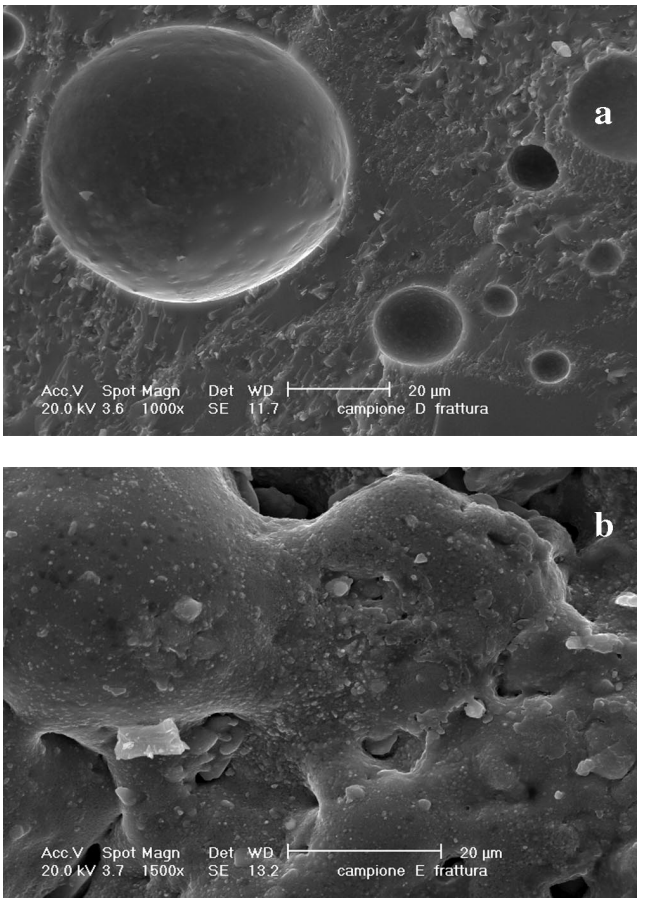


**Fig. 6.** SEM image of fractured G1-air (a) and G1-$N_2$ (b) glass-ceramics.

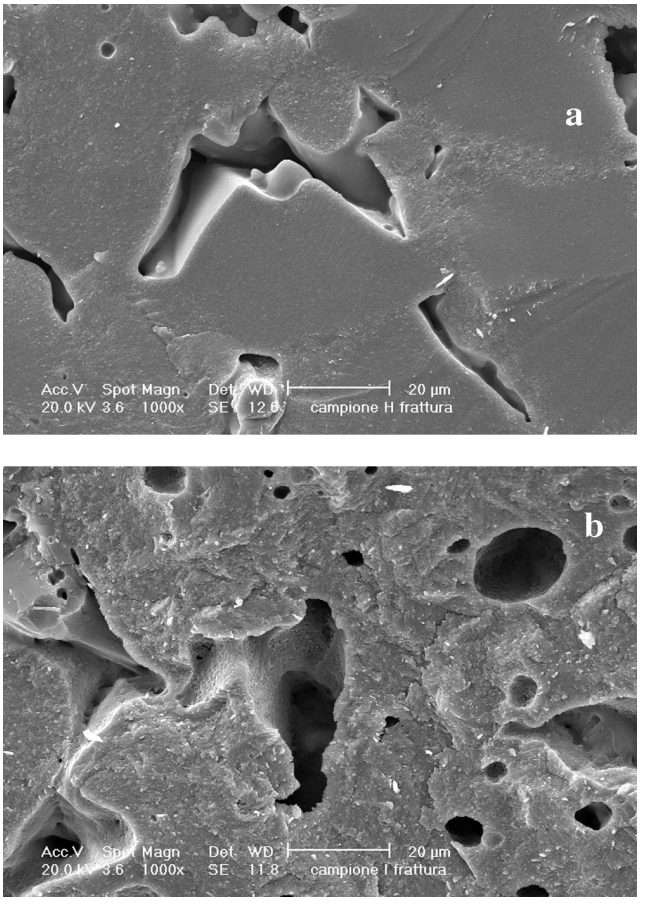


**Fig. 7.** SEM image of fractured G2-air (a) and G2-$N_2$ (b) glass-ceramics.

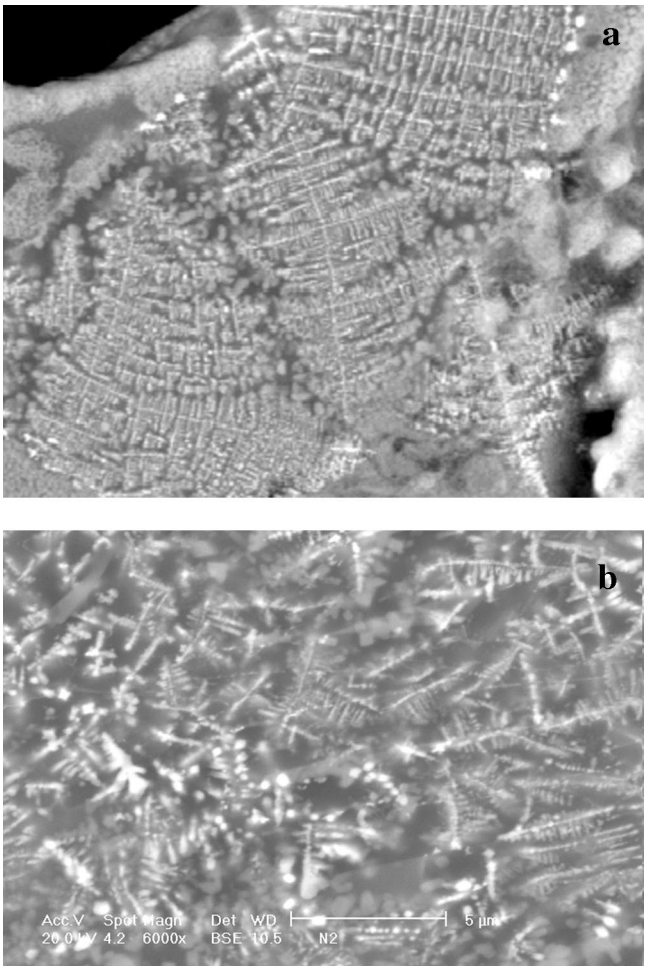


**Fig. 8.** SEM image obtained by BSE on polished G2-air (a) and G2-$N_2$ (b) samples.

The XRD spectra of the sintered glass-ceramics (Fig. 5) show that the crystalline-phase formation is higher in $N_2$ atmosphere. The degree of crystallinity is 41 ± 3 wt% in G1-$N_2$ and 28 ± 3% in G1-air; in G2-$N_2$ and G2-air the amount of crystal phase formed is 57 ± 3 wt% and 48 ± 3%, respectively. The comparison of the G1 spectra highlights that the higher crystallinity of the sample sintered in $N_2$ is due to the increase of both magnetite and pyroxene phases. By comparing G2 spectra, it turns out that only the magnetite peak increases, which can be explained by considering that in G2 the iron oxides content is higher than in G1. The intensive magnetite formation justifies the high-crystallization trend of the G2-$N_2$ sample.

In the previous work,[19] the structure of G1 and G2 was investigated after 1-h holding in air at different temperatures. It was demonstrated that, in G1-air, due to the low percentage of the crystal phase formed, the sintering starts at 900°C; at 950°C a closed porosity is formed, and at 1000°C the pore coalescence takes place. The densification of G2-air starts at 1000°C, and the final structure, at 1050°C, is characterized by open porosity.

In the present study, the structures of the final glass-ceramics, sintered in air and in nitrogen atmospheres, are compared. Figures 6 and 7 show the fractures of G1-air (Fig. 6(a)) and G1-$N_2$ (Fig. 6(b)), and G2-air (Fig. 7(a)) and G2-$N_2$ (Fig. 7(b)), respectively. Figure 8 highlights the crystal morphology of G2-air (Fig. 8(a)) and G2-$N_2$ (Fig. 8(b)) obtained by BSE observation. Due to the lower sintering temperature, in G1-$N_2$ no closed porosity and pore coalescence is observed (as in G1-air); the structure shows an open porosity with consistent neck growths. In G2-air and G2-$N_2$ the structures of the final glass-ceramics are similar. This may be explained by the higher crystallization ability of G2 compared with G1 and the consequent higher sintering temperatures.

The BSE study of G2-air and G2-$N_2$ shows the typical pyroxene dendrite crystal structure and highlights that the crystal size is smaller in the nitrogen atmosphere heat-treatment; this phenomenon might be related to the intensive magnetite bulk nucleation.

The mechanical properties were measured using a series of five samples, obtained after 1-h isothermal step in air and nitrogen atmospheres. Table II summarizes the sintering teperatures, the shrinkage values, and the experimentally measured property. The results demonstrate that better properties are obtained in $N_2$ atmosphere, especially the bending strength notwithstanding the lower sintering temperatures. This was explained by the higher percentage of crystal phase formed in the $N_2$-sintered samples and the finer crystalline structure.

## IV. Conclusions

In nitrogen atmospheres, the sintering of iron-rich glass-ceramics occurs at 100°–200°C lower temperature, which is explained by the absence of $Fe^{2+}$ oxidation and the lower viscosity of the parent and residual glasses.

The higher amount of crystal phase and the finer crystalline dendrite structure, obtained during the heat-treatment in inert atmosphere, improves the mechanical properties of the sintered glass-ceramics.

## References

[1]J. Hlavac, *The Technology of Glass and Ceramics: An Introduction*; p. 32. Elsevier, Amsterdam, Netherlands, 1983.

[2]J. Williamson, A. J. Tipple, and P. S. Rogers, "Influence of Iron Oxides on Kinetics of Crystal Growth in CaO–MgO–$Al_2O_3$–$SiO_2$ Glasses," *J. Iron Steel Inst., London*, [Sept] 898–903 (1968).

[3]N. M Pavlushkin, *Chemical Technology of Glass and Sitalls (Russian)*; Stroiizdat, Moscow, Russia, 1983.

[4]A. Karamanov, P. Pisciella, C. Cantalini, and M. Pelino, "The Influence of the $Fe^{3+}/Fe^{2+}$ Ratio on the Crystallization of Iron-Rich Glasses from Industrial Wastes," *J. Am. Ceram. Soc.*, **83** [12] 3153–57 (2000).

[5]H. Beall and H. L. Rittler, "Basalt Glass Ceramics," *Am. Ceram. Soc. Bull.*, **55** [6] 579–82 (1976).

[6]D. J. Burkhard, "Iron-Bearing Silicate Glasses at Ambient Conditions," *J. Non-Cryst. Solids*, **275**, 175–88 (2000).

[7]C. G. Rouse and J. Williamson "Semiconducting Glass-Ceramics in the System CaO–MgO–$Al_2O_3$–$SiO_2$ with Added Iron Oxides"; pp. 91–105 in *Congress of Special Ceramics*. British Ceramic Research Association, Penkhull, Great Britain, 1975.

[8]W. Holand and G. Beall, *Glass-Ceramics Technology*; pp. 162–67. The American Ceramics Society, Westerville, OH, 2002.

[9]A. Karamanov and M. Pelino M., "Crystallization Phenomena in Iron Rich Glasses," *J. Non-Cryst. Solids*, **281** [1–3] 139–51 (2001).

[10]M. Romero and J. Ma, Rincon, "Preparation and Properties of High Iron Content Glasses Obtained from Industrial Wastes," *J. Eur. Ceram. Soc.*, **18**, 153–60 (1998).

[11]D. Schreiber, B. K. Kochanowski,and C. W. Shreberg, "Compositional Effect on the Iron Redox State in Model Glasses for Nuclear Waste Immobilization"; pp. 141–50 in Ceramic Transctions, Vol. 39, *Environmental and Waste Management Issues in the Ceramic Industry*. Edited by G. B. Mellinger. The American Ceramic Society, Westerville, OH, 1994.

[12]I. Vicente-Mingarro, J. Ma. Rincon, P. Bowles, R. D. Rawlings, and P. S. Rogers, "Viscosity Measurements on Glass Obtained from Alkaline Volcanic Rocks of the Canary Island," *Glass Technol.*, **33** [2] 49–52 (1992).

[13]A. Karamanov, R. Di Gioacchino, P. Pisciella, and M. Pelino, "Viscosity of Iron-Rich Glasses from Industrial Wastes," *Glass Technol.*, **43** [1] 34–38 (2002).

[14]B. Locsei, *Molten Silicates and Their Properties.* Akademiai Kiado, Budapest, Hungary, 1970.

[15]R. D. Cooper, J. B. Fanselow, and D. B. Poker, "The Mechanism of Oxidation of a Basaltic Glass: Chemical Diffusion of Network-Modifying Cations," *Geochim. Cosmochim. Acta*, **60** [17] 3253–65 (1996).

[16]M. Romero, and J. Ma, Rincon, "Surface and Bulk Crystallization of Glass-Ceramics in the $Na_2O$–CaO–ZnO–PbO–$Fe_2O_3$ System Derived from a Goethite Waste," *J. Am. Ceram. Soc.*, **82** [5] 1313–17 (1999).

[17]A. Karamanov, G. Taglieri, and M. Pelino, "Iron-Rich Sintered Glass-Ceramics from Industrial Wastes," *J. Am. Ceram. Soc.*, **82** [11] 3012–16 (1999).

[18]D. J. Burkhard, "Crystallization and Oxidation of Kilauea Basal Glass: Processes during reheating Experiments," *J. Petrol.*, **42** [3] 507–27 (2001).

[19]A. Karamanov and M. Pelino, "Sintering Behavior and Properties of Iron-Rich Glass-Ceramics," *J. Am. Ceram. Soc.*, in press.

[20]Z. Strnad, *Glass-Ceramic Materials*; p. 160. Elsevier, Amsterdam, Netherlands, 1986.

[21]A. Karamanov, P. Pisciella, and M. Pelino, "The Crystallisation Kinetics of Iron Rich Glasses in Different Atmospheres," *J. Eur. Ceram. Soc.*, **20** [12] 2233–37 (2000).

[22]W. Deer, R. Howie, and J. Zussman, *An Introduction to the Rock-Forming Minerals*, 2nd ed.; pp. 541–62. Longman Scientific & Technical, Essex, U.K., 1992. □